

Article

## Limit Cycles in Nonlinear Systems with Fractional Order Plants

Derek P. Atherton <sup>1</sup>, Nusret Tan <sup>2,\*</sup>, Celaledin Yeroglu <sup>3</sup>, Gürkan Kavuran <sup>4</sup> and Ali Yüce <sup>2</sup>

<sup>1</sup> School of Engineering and Informatics, Department of Engineering and Design, Sussex University, Brighton, BN1 9QT, UK; E-Mail: d.p.atherton@sussex.ac.uk

<sup>2</sup> Department of Electrical and Electronics Engineering, İnönü University, Malatya 44280, Turkey; E-Mail: ali.yuce@inonu.edu.tr

<sup>3</sup> Department of Computer Engineering, İnönü University, Malatya 44280, Turkey; E-Mail: c.yeroglu@inonu.edu.tr

<sup>4</sup> Department of Mechatronics Engineering, Fırat University, Elazığ 23100, Turkey; E-Mail: gkavuran@firat.edu.tr

\* Author to whom correspondence should be addressed; E-Mail: nusret.tan@inonu.edu.tr; Tel.: +90-422-377-4826; Fax: +90-422-341-0046.

Received: 31 March 2014; in revised form: 9 June 2014 / Accepted: 1 July 2014 /

Published: 17 July 2014

---

**Abstract:** In recent years, there has been considerable interest in the study of feedback systems containing processes whose dynamics are best described by fractional order derivatives. Various situations have been cited for describing heat flow and aspects of bioengineering, where such models are believed to be superior. In many situations these feedback systems are not linear and information on their stability and the possibility of the existence of limit cycles is required. This paper presents new results for determining limit cycles using the approximate describing function method and an exact method when the nonlinearity is a relay characteristic.

**Keywords:** Tsytkin locus;  $A$  function; fractional order systems; nonlinear systems with fractional order plants; describing function; limit cycles

---

### 1. Introduction

In recent years, there has been considerable interest in the study of feedback systems containing processes whose dynamics are best described by fractional order derivatives. A physical system

represented by a differential equation where the orders of derivatives can take any real number and not necessarily an integer number can be called a fractional order system. The idea of non-integer order (or fractional order) differentiation/integration emerged in 1695 [1]. At the beginning, mathematicians studied it only as a theoretical subject due to its complexity and therefore other science disciplines could not use it effectively owing to the absence of exact solution methods of non-integer order differential equations [2]. However, in recent years, facilitated by today's computational facilities, considerable attention has been given to fractional order systems, including fractional order control systems.

Interest in fractional calculus has made a significant impact on the field of control engineering and as a result of this there have been many studies dealing with the analysis and design of control systems. It has been seen that the frequency domain approaches of classical control, where the Laplace complex variable of a transfer function is replaced by  $j\omega$ , such as Bode, Nyquist and Nichols diagrams can be applied to a fractional order plant without any modification. However, for time domain analysis integer approximations of fractional powers of  $s$ , such as given in [3–6], which are not exact have to be used. On the design side, fractional order versions of classical controllers, such as fractional order PID, have been designed [7] and applied [8–11] and various results have been obtained for stability analysis [12,13]. However, the field of fractional order control systems still needs further research on many important problems. One of these situations is when nonlinearity occurs in a control system. It is well known that all practical systems are nonlinear and linear models of many engineering systems are always approximate [14]. It is apparent, since as mentioned above the frequency domain representation of a fractional order plant is exact, that frequency domain methods can play an important role in analysis and design.

The aim of this paper is to study the problem of the stability of an autonomous nonlinear feedback system with a fractional order plant. The stability of a nonlinear control system can often be demonstrated by showing that there is no possibility of the existence of sustained oscillations, known as limit cycles. The most powerful, although approximate, method for such investigations is the Describing Function (DF) method [15, 16]. The frequency at the intersection point, when one exists, of the Nyquist plot of the system and the complex plot of the negative inverse of the DF is used in limit cycle analysis. A review of the classical DF method is given and application to a control system with a fractional order plant is demonstrated. Tsypkin [17] presented a frequency domain method for the exact analysis of limit cycles in relay feedback systems and the problem is formulated in terms of  $A$  loci [14], which are frequency dependent loci and more general than the Tsypkin loci. A program is developed in MATLAB for computation of limit cycles by the Tsypkin method in a feedback loop with an on–off relay, relay with hysteresis or relay with dead zone and a fractional order plant.

The rest of the paper is organized as follows: A review of fractional order dynamics is given in Section 2. Section 3 studies stability and limit cycles in nonlinear systems with FOTF. The DF analysis for nonlinear fractional order control systems is given. Computation of the  $A$  locus of a fractional order plant and some examples are presented for limit cycles in relay systems. Section 4 gives some concluding remarks.

## 2. Fractional Order Dynamics

Many real systems are known to display fractional order dynamics. For example, it is known that the semi-infinite lossy (RC) transmission line demonstrates fractional behavior since the current into the line is equal to the half derivative of the applied voltage that is  $V(s) = (1/\sqrt{s})I(s)$  [18]. Thus, the significance of fractional order representation is that fractional order differential equations are more adequate to describe some real world systems than those of integer order models [19,20]. Many physical systems such as viscoelastic materials [21,22], electromechanical processes [23], long transmission lines [24], dielectric polarisations [25], colored noise [26], cardiac behavior [27], problems in bioengineering [28], and chaos [29] can be described using fractional order differential equations. Thus, fractional calculus has been an important tool to be used in engineering, chemistry, physical, mechanical and other sciences. Extensive results on fractional order systems and control can be found in the book by Monje *et al.* [30].

Fractional order calculus is a generalization of the ordinary differentiations by non-integer derivatives. Many mathematicians like Liouville and Riemann contributed to the field of fractional calculus. There are different definitions of fractional order operators such as Grünwald-Letnikov, Riemann-Liouville and Caputo [31]. The Caputo definition can be stated as [32],

$$L\{D^\alpha y(t)\} = s^\alpha L\{y(t)\} - \sum_{i=0}^{[\alpha]-1} s^{\alpha-i-1} \frac{d^i y}{dt^i}(0) \quad (1)$$

where  $D^\alpha y(t) = d^\alpha y(t)/dt^\alpha$  indicates the Caputo derivative of  $y(t)$ ,  $\alpha \in R_+$  is the rational number,  $[\alpha]$  is the integer part of  $\alpha$  and  $L$  denotes the Laplace transform.

A fractional order control system with input  $r(t)$  and output  $y(t)$  can be described by a fractional differential equation of the form [33],

$$\begin{aligned} & a_n D^{\alpha_n} y(t) + a_{n-1} D^{\alpha_{n-1}} y(t) + \dots + a_0 D^{\alpha_0} y(t) \\ & = b_m D^{\beta_m} r(t) + b_{m-1} D^{\beta_{m-1}} r(t) + \dots + b_0 D^{\beta_0} r(t) \end{aligned} \quad (2)$$

or by a fractional order transfer function of the form,

$$G(s) = \frac{Y(s)}{R(s)} = \frac{b_m s^{\beta_m} + b_{m-1} s^{\beta_{m-1}} + \dots + b_0 s^{\beta_0}}{a_n s^{\alpha_n} + a_{n-1} s^{\alpha_{n-1}} + \dots + a_0 s^{\alpha_0}} \quad (3)$$

where  $a_i, b_j$  ( $i = 0, 1, 2, \dots, n$  and  $j = 0, 1, 2, \dots, m$ ) are real parameters and  $\alpha_i, \beta_j$  are real positive numbers and  $\alpha_0 < \alpha_1 < \dots < \alpha_n$  and  $\beta_0 < \beta_1 < \dots < \beta_m$ . Thus, a transfer function including fractional powered  $s$  terms can be called a fractional order transfer function, FOTF. For example, with the FOTF  $G(s) = 1/(s^{2.3} + 2s^{0.7} + 1)$  replacing  $s$  by  $j\omega$  and using  $(j\omega)^\alpha = \omega^\alpha (\cos \alpha\pi/2 + j \sin \alpha\pi/2)$ , one obtains

$$G(j\omega) = \frac{1}{(1 + 0.9080\omega^{0.7} - 0.8910\omega^{2.3}) + j(1.7820\omega^{0.7} - 0.4540\omega^{2.3})} \quad (4)$$

Bode and Nyquist diagrams of this equation can then be obtained as shown in Figures 1 and 2. This example is given to show that the frequency response computation of FOTF can be obtained similar to integer order transfer functions. However, for time domain computation, there is not a general analytical method for determining the output of a control system with an FOTF. There have been many

studies over the years [34–36], some of them are based on integer approximation models and others based on numerical approximation of the non-integer order operator. The methods developing integer order approximations can be used for time domain analysis of fractional order control systems similar to classical control approaches. Some of the well known methods for evaluating rational approximations are the Continued Fractional Expansion (CFE) method, Oustaloup's method, Carlson's method, Matsuda's method, Chareff's method, least square methods and others [18, 37–41].

**Figure 1.** Bode plots of Equation (4).

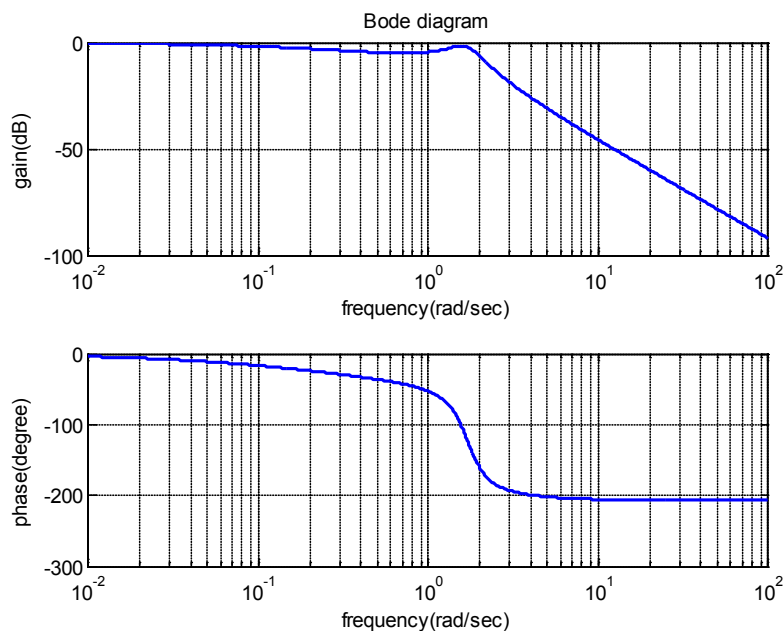
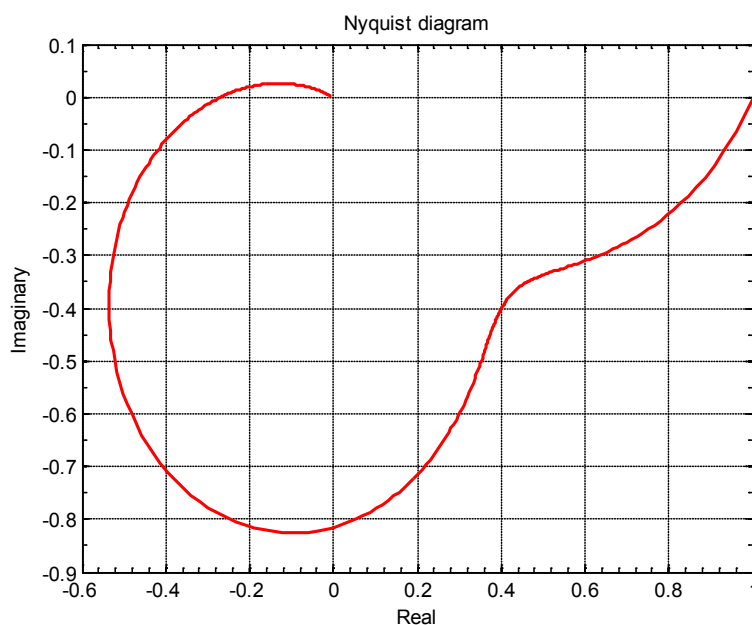


**Figure 2.** Nyquist plot of Equation (4).



In this paper, the CFE method given in [35,42] is used for time domain simulation of nonlinear control systems with FOTF. This method finds approximations from

$$(1+x)^\alpha \cong \frac{1}{1-1} + \frac{\alpha x}{1+} + \frac{(1+\alpha)x}{2+} + \frac{(1-\alpha)x}{3+} + \frac{(2+\alpha)x}{2+} + \frac{(2-\alpha)x}{5+\dots} \quad (5)$$

where  $x = s - 1$ . Thus, first, second, third and fourth integer order approximations of  $s^\alpha$  can be found from the following equations

$$s^\alpha \cong \frac{(1+\alpha)s + (1-\alpha)}{(1-\alpha)s + (1+\alpha)} \quad (6)$$

$$s^\alpha \cong \frac{(\alpha^2 + 3\alpha + 2)s^2 + (-2\alpha^2 + 8)s + (\alpha^2 - 3\alpha + 2)}{(\alpha^2 - 3\alpha + 2)s^2 + (-2\alpha^2 + 8)s + (\alpha^2 + 3\alpha + 2)} \quad (7)$$

$$s^\alpha \cong \frac{(\alpha^3 + 6\alpha^2 + 11\alpha + 6)s^3 + (-3\alpha^3 - 6\alpha^2 + 27\alpha + 54)s^2 + (3\alpha^3 - 6\alpha^2 - 27\alpha + 54)s + (-\alpha^3 + 6\alpha^2 - 11\alpha + 6)}{(-\alpha^3 + 6\alpha^2 - 11\alpha + 6)s^3 + (3\alpha^3 - 6\alpha^2 - 27\alpha + 54)s^2 + (-3\alpha^3 - 6\alpha^2 + 27\alpha + 54)s + (\alpha^3 + 6\alpha^2 + 11\alpha + 6)} \quad (8)$$

$$s^\alpha \cong \frac{(\alpha^4 + 10\alpha^3 + 35\alpha^2 + 50\alpha + 24)s^4 + (-4\alpha^4 - 20\alpha^3 + 40\alpha^2 + 320\alpha + 384)s^3 + (6\alpha^4 - 150\alpha^2 + 864)s^2 + (-4\alpha^4 + 20\alpha^3 + 40\alpha^2 - 320\alpha + 384)s + (\alpha^4 - 10\alpha^3 + 35\alpha^2 - 50\alpha + 24)}{(\alpha^4 - 10\alpha^3 + 35\alpha^2 - 50\alpha + 24)s^4 + (-4\alpha^4 + 20\alpha^3 + 40\alpha^2 - 320\alpha + 384)s^3 + (6\alpha^4 - 150\alpha^2 + 864)s^2 + (-4\alpha^4 - 20\alpha^3 + 40\alpha^2 + 320\alpha + 384)s + (\alpha^4 + 10\alpha^3 + 35\alpha^2 + 50\alpha + 24)} \quad (9)$$

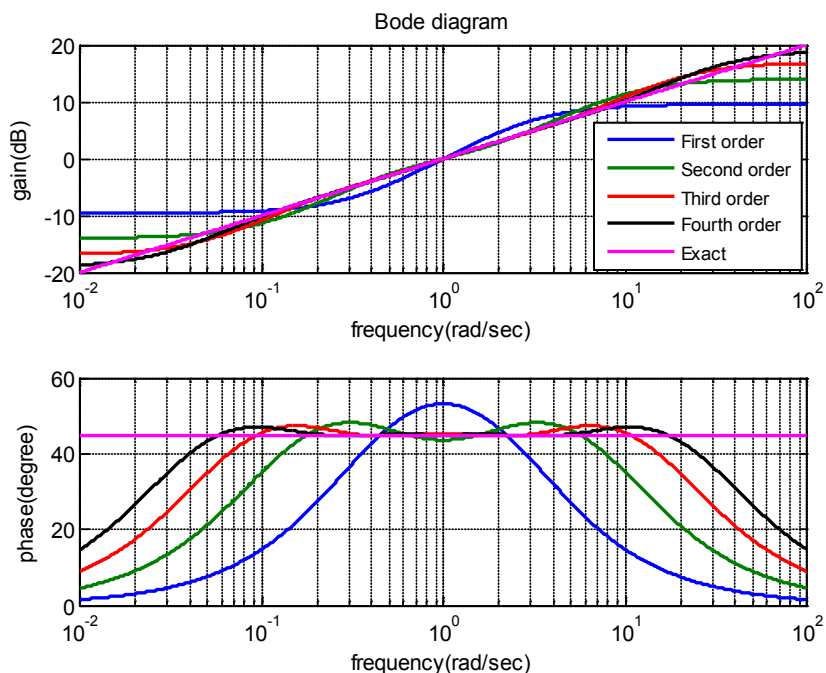
The fourth order approximation has been used for the simulations reported in this paper. The following examples show that the fourth order approximations given in Equation (9) give good results.

The Bode plots of first, second, third, fourth order approximations of  $G(s) = s^{0.5}$  and its exact Bode plots are shown in Figure 3 where it can be seen that the fourth order Bode plots fit with the exact Bode plots for the frequencies approximately from 0.04 rad/s to 20 rad/s. The step responses for  $G(s) = 1/(s^{1.5} + 1)$  using first, second, third and fourth order approximations for  $s^{0.5}$  are given in Figure 4. The third and fourth order approximations match almost exactly. One of the most well-known approximation techniques is Oustaloup's method [37]. Oustaloup's method gives 1,3,5,7,... order integer approximations. A comparison between approximations given in Equation (9) and Oustaloup's method for  $G(s) = 1/(s^{1.5} + 1)$  is given in Figure 5. The comparison is done between the seventh order Oustaloup's approximation and the fourth order approximation given in Equation (9). The seventh order Oustaloup's approximation for  $s^{0.5}$  is

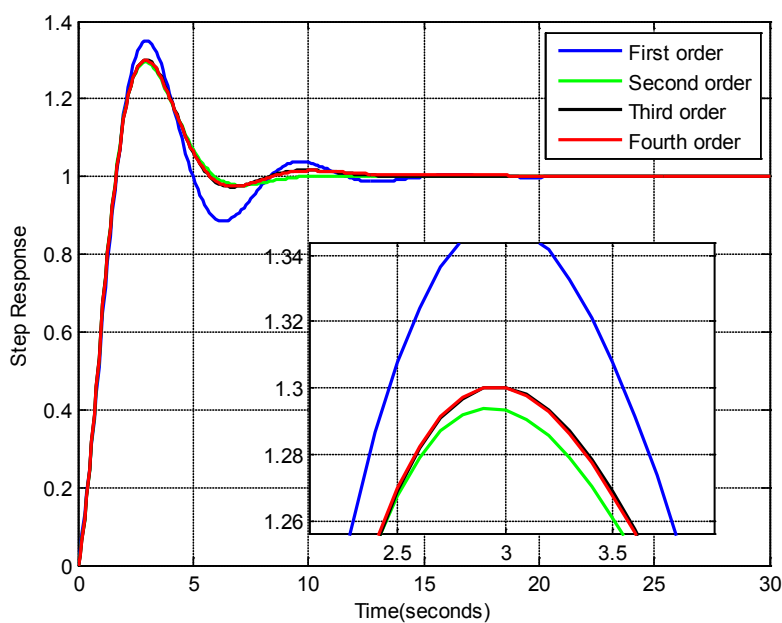
$$s^{0.5} \cong \frac{10s^7 + 509.4s^6 + 5487s^5 + 14990s^4 + 10790s^3 + 2045s^2 + 98.34s + 1}{s^7 + 98.34s^6 + 2045s^5 + 10790s^4 + 14990s^3 + 5487s^2 + 509.4s + 10} \quad (10)$$

Figure 5 shows that two step responses agree very closely. However, we prefer to use the fourth order approximation given in Equation (9) since Oustaloup’s approximation is seventh order. Also in [35] it has been shown that the approximations given in Equations (6)–(9) provide very good results.

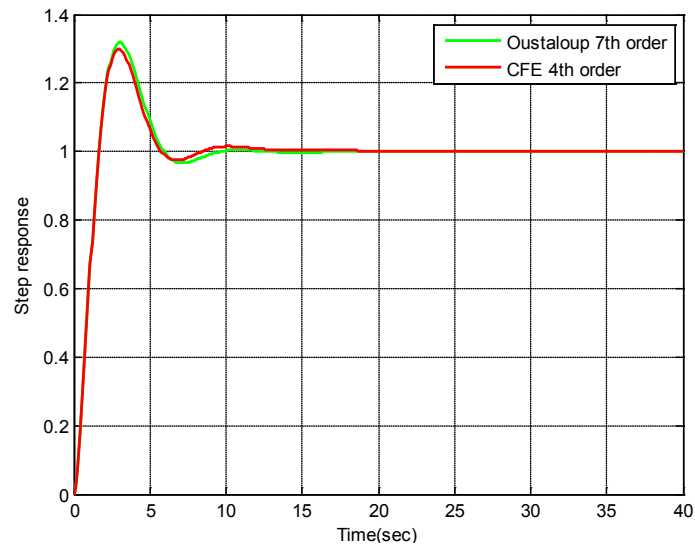
**Figure 3.** Exact Bode plots of  $s^{0.5}$  and first, second, third, fourth order approximations.



**Figure 4.** Step responses for  $G(s) = 1/(s^{1.5} + 1)$  using first, second, third and fourth order approximations given in Equations (6)–(9).



**Figure 5.** Step responses using the fourth order approximation given in Equation (9) and seventh order Oustaloup approximation.



### 3. Determination of Stability and Limit Cycles in Nonlinear Systems

#### 3.1. Describing Function Method

The DF,  $N(a)$ , of a nonlinear element is defined as the ratio of the fundamental output to the magnitude of an applied sinusoidal input [43]. Considering a nonlinear element  $n(x)$  with input  $x = a \sin \theta$  and corresponding output  $y(\theta)$ , then if  $n(x)$  has odd symmetry, the fundamental component in  $y(\theta)$ , namely  $b_1 \sin \theta + a_1 \cos \theta$ , has

$$b_1 = \frac{2}{\pi} \int_0^{\pi} y(\theta) \sin \theta d\theta \quad (11)$$

$$a_1 = \frac{2}{\pi} \int_0^{\pi} y(\theta) \cos \theta d\theta \quad (12)$$

The describing function  $N(a)$  is then given by

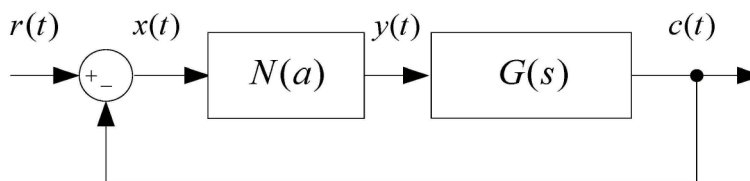
$$N(a) = (b_1 + ja_1)/a \quad (13)$$

which will be real, that is,  $a_1 = 0$ , if the nonlinearity is single valued. To investigate the possibility of a limit cycle in the system of Figure 6 the characteristic equation

$$1 + N(a)G(s)|_{s=j\omega} = 0 \quad (14)$$

is then examined. Typically, this is done using a Nyquist diagram where the loci  $G(j\omega)$  and  $C(a) = -1/N(a)$  are plotted, and any intersection of the loci gives the amplitude and frequency of a possible limit cycle. Fortunately, the frequency domain analysis of a FOCS (Fractional Order Control System) can be conducted in a similar way to that of an integer order one. Therefore, the frequency domain expression can be easily obtained by substituting  $s = j\omega$  in the Laplace transform of the transfer function. Since the describing function method is a frequency domain approach, it can be applied to the FOCS to analyze some aspects of the effect of nonlinearity on its performance.

Figure 6. A simple nonlinear feedback system.



When the nonlinearity in the negative unity feedback control system of Figure 6 is an ideal relay or relay with hysteresis as shown in Figures 7 and 8 nonlinearity then their DFs are respectively:

$$N(a) = \frac{4h}{\pi a} \quad \text{and} \quad N(a) = \frac{4h(a^2 - \Delta^2)^{1/2}}{a^2\pi} - j \frac{4h\Delta}{a^2\pi} \tag{15}$$

The possibility of a limit cycle can then be investigated as shown in the following example.

**Example 1:** Consider the control system of Figure 6 with the following fractional order plant

$$G_1(s) = \frac{4}{s^{0.7}(s + 1)^2} = \frac{4}{s^{2.7} + 2s^{1.7} + s^{0.7}} \tag{16}$$

Figure 7. The diagram of the ideal relay.

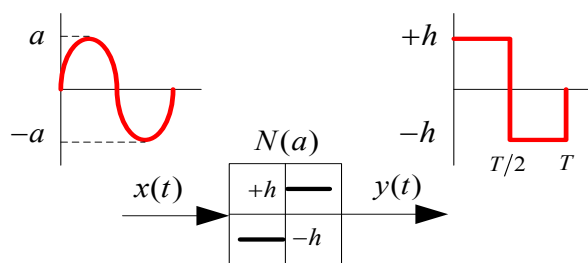


Figure 8. The diagram of the relay with hysteresis.

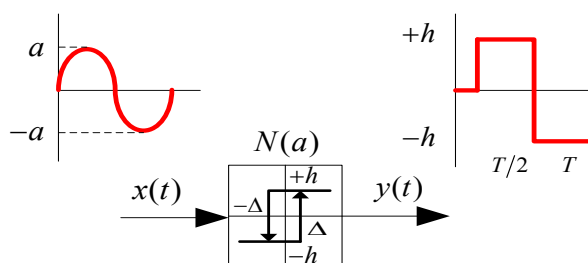


Figure 9 presents the Nyquist plot of the plant  $G(s)$  and the negative inverse of the describing function in Equation (15).

From Figure 9, a limit cycle of frequency  $\omega = 1.632$  rad/s is predicted for the fractional order system. Since  $N(a) = 4h/\pi a$  for the ideal relay nonlinearity, for  $h = 1$ , the approximate amplitude of the limit cycle can be calculated from the intersection point of  $G(j\omega)$  and  $C(a)$  as,

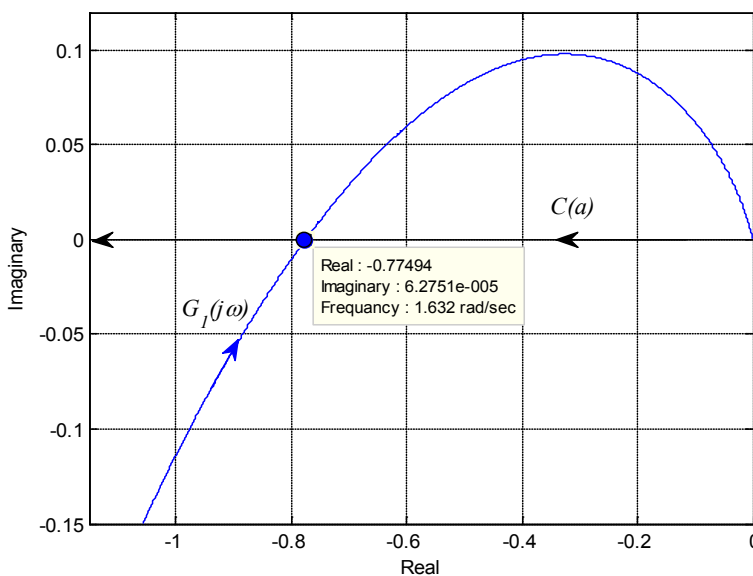
$$G(j\omega) = -\frac{1}{N(a)} = C(a) \tag{17}$$

$$-0.774 = -\frac{\pi a}{4} \rightarrow a = 0.985$$

This amplitude, according to DF theory, is an approximation for the amplitude of the fundamental, although it is often assumed for convenience to be the amplitude of the distorted limit cycle. The period of the oscillation is given by;

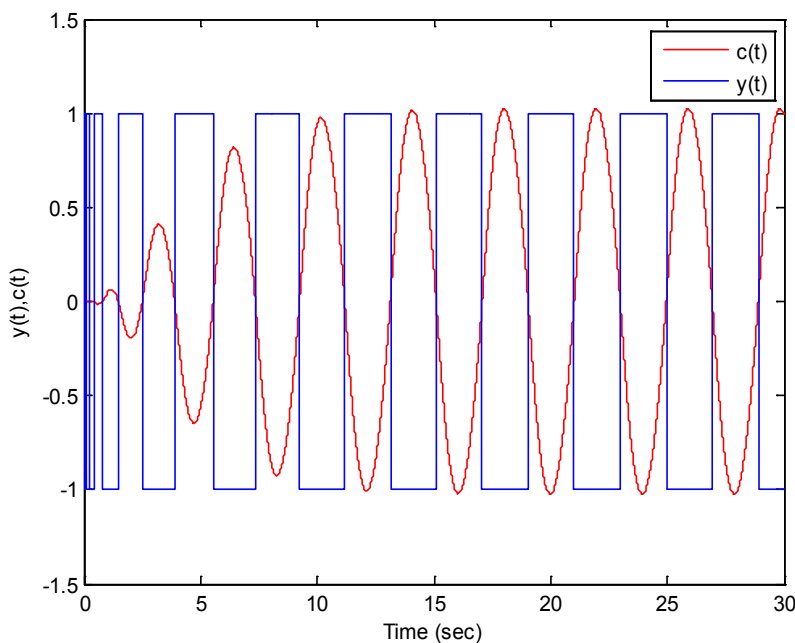
$$\omega = 2\pi \frac{1}{T}; 1.632 = \frac{2\pi}{T} \rightarrow T = 3.84 \text{ s} \tag{18}$$

**Figure 9.** Nyquist diagram of  $G_1(j\omega)$  and plot of  $C(a)$ .



The simulation results for the nonlinear control system with the relay nonlinearity are given in Figure 10. The simulation results, for which the measured peak amplitude and period were 1.025 and 3.93 s respectively, agree well with the DF analysis method although both are approximate. As the limit cycle is near to sinusoidal, the DF result may be expected to be quite accurate.

**Figure 10.** Time responses of closed loop system in Figure 6 with  $G_1(j\omega)$  and ideal relay.



### 3.2. Tsytkin's Method

The analysis of the relay feedback problem can be studied using the frequency domain approach of the Tsytkin method and the  $A$  Loci approach [14]. For a feedback loop containing a relay and a transfer function  $G(s)$ , limit cycles can be found using the  $A$  loci of  $G(s)$  where

$$A_G(\theta, \omega) = \text{Re}A_G(\theta, \omega) + j\text{Im}A_G(\theta, \omega) \quad (19)$$

with

$$\text{Re}A_G(\theta, \omega) = \sum_{n=1}^{\infty} V_G(n\omega) \sin n\theta + U_G(n\omega) \cos n\theta \quad (20)$$

and

$$\text{Im}A_G(\theta, \omega) = \sum_{n=1}^{\infty} (1/n)[V_G(n\omega) \cos n\theta - U_G(n\omega) \sin n\theta] \quad (21)$$

where  $G(jn\omega) = U_G(n\omega) + jV_G(n\omega)$ .  $A_G(\theta, \omega)$  is a generalized summed frequency locus with its real and imaginary values at a particular frequency,  $\omega$ , depending on weighted values, according to the choice of  $\theta$ , of the real and imaginary values of  $G(j\omega)$  at the frequencies  $n\omega$  for  $n = 1, 2, \dots, \infty$ . In particular, for  $\theta = 0$  the real (imaginary) part of  $A_G(\theta, \omega)$  depends only upon the real (imaginary) part of  $G(j\omega)$  at frequencies  $n\omega$ . It is possible to evaluate  $\text{Re}A_G(\theta, \omega)$  and  $\text{Im}A_G(\theta, \omega)$  by computationally summing to a finite number,  $M$ , of terms. For integer transfer functions, closed form solutions have been found for the infinite series but this remains an open problem for fractional order transfer functions (FOTFs). When the limit cycle is odd symmetrical only odd values of  $n$  are required in the series and the corresponding  $A$  locus is denoted by  $A^o$ . Some properties of the  $A$  loci are:

$$\frac{d \text{Im}[A_G(\theta, \omega)]}{d\theta} = -\text{Re}A_G(\theta, \omega) \quad (22)$$

The  $A^o$  locus for  $\theta = 0$  is identical with the Tsytkin locus [17],  $\Lambda(\omega)$ , if  $\lim_{s \rightarrow \infty} sG(s) = 0$ , apart from a constant factor. The relationship is

$$\Lambda(\omega) = (4h/\pi)A^o(0, \omega) \quad (23)$$

The  $A^o$  locus can thus be regarded as a generalized Tsytkin locus. The  $A$  locus satisfies the superposition property, that is if the linear plant  $G(s) = G_1(s) + G_2(s)$ , then

$$A_G(\theta, \omega) = A_{G_1}(\theta, \omega) + A_{G_2}(\theta, \omega) \quad (24)$$

If  $G_1(s) = G(s)e^{-s\tau}$ , then

$$A_{G_1}(\theta, \omega) = A_G(\theta + \omega\tau, \omega) \quad (25)$$

The loci are periodic in  $\theta$ , with period  $2\pi$ , that is

$$A_G(\theta, \omega) = A_G(\theta + 2\pi, \omega) \quad (26)$$

For  $A^o$  the periodicity is odd, that is

$$A_G^o(\theta, \omega) = -A_G^o(-\theta, \omega) \quad (27)$$

Since any integer plant transfer function can be written in terms of a summation of transfer functions having a real or complex pair of poles, use of Equation (24) allows  $A$  loci for most integer transfer functions to be obtained in terms of the  $A$  loci of a few basic transfer functions.

For a relay with no dead zone, the simplest assumption for the periodic output is a square wave with 1:1 mark space ratio. By taking the Fourier series for the square wave and calculating the corresponding series for the output of  $G$  it can be shown that the output and the derivative of the output of the linear transfer function  $G$  can be expressed in terms of the  $A$  loci [14]. This also applies to the situation where the relay has dead zone, where unlike the situation for the relay without dead zone, finite values of  $\theta$  are required. Taking the input to the relay,  $x(t) = -c(t)$ , where  $c(t)$  is the output of  $G(s)$ , and assuming the relay to have a hysteresis of  $\pm\Delta$ , that is it switches from  $-h$  to  $+h$  for an input of  $\Delta$  at time zero and from  $+h$  to  $-h$  for an input of  $-\Delta$ , the switching condition

$$x(0) = \Delta \quad \text{and} \quad \dot{x}(0) > 0 \quad (28)$$

yields the result

$$\text{Im}A_G^o(0, \omega) = -\pi\Delta/4h \quad \text{and} \quad \text{Re}A_G^o(0, \omega) < 0 \quad (29)$$

provided  $\lim_{s \rightarrow \infty} sG(s) = 0$ . When the latter is not the case, discontinuities in the relay input or its derivative may occur at the switching instants and known corrections need to be applied to the equations.

For a relay with dead zone the solution is obtained from

$$\text{Im}A_G^o(0, \omega) - \text{Im}A_G^o(\omega\Delta t, \omega) = -(\pi/2h)(\delta + \Delta) \quad (30)$$

$$\text{Re}A_G^o(0, \omega) - \text{Re}A_G^o(\omega\Delta t, \omega) < 0 \quad (31)$$

and

$$\text{Im}A_G^o(0, \omega) - \text{Im}A_G^o(-\omega\Delta t, \omega) = (\pi/2h)(\delta - \Delta) \quad (32)$$

$$\text{Re}A_G^o(0, \omega) - \text{Re}A_G^o(-\omega\Delta t, \omega) < 0 \quad (33)$$

Here, there are two equations as there are two unknowns the pulse width,  $\Delta t$ , and the limit cycle frequency,  $\omega$ . Note the expressions involving the real parts need not normally be checked but it is easily done if the solutions are obtained graphically by plotting for the relay with no dead zone  $A_G^o(0, \omega)$  and for the relay with dead zone  $A_G^o(0, \omega) - A_G^o(\omega\Delta t, \omega)$  and  $A_G^o(0, \omega) - A_G^o(-\omega\Delta t, \omega)$ . Consider the transfer function  $G(s) = 1/s(s+1)(s+2)$  in a feedback loop having a relay with hysteresis. For this transfer function

$$G(j\omega) = \frac{1}{j\omega(1+j\omega)(2+j\omega)} = \frac{-3\omega^2}{(-3\omega^2)^2 + (2\omega - \omega^3)^2} - \frac{j(2\omega - \omega^3)}{(-3\omega^2)^2 + (2\omega - \omega^3)^2} \quad (34)$$

thus for an odd symmetrical limit cycle

$$A_G^o(0, \omega) = \sum_{n=1(2)}^{\infty} U_G(n\omega) + j[V_G(n\omega)/n] = \sum_{n=1(2)}^{\infty} \frac{-3n^2\omega^2}{(-3n^2\omega^2)^2 + (2n\omega - n^3\omega^3)^2} - \frac{j(2n\omega - n^3\omega^3)}{n[(-3n^2\omega^2)^2 + (2n\omega - n^3\omega^3)^2]} \quad (35)$$

The limit cycle solution frequency is given where the above locus meets the line  $-\pi\Delta/4h$  parallel to the negative real axis on a Nyquist plot. The DF solution is given where  $G(j\omega)$  meets this line, so when a program is written where  $n$  can be input then the DF solution can be obtained for  $n = 1$  and convergence can be seen by taking larger and larger values of  $n$ . Thus, plotting  $A_G^0(0, \omega)$  and  $G(j\omega)$  provides a good graphical approach for obtaining the limit cycle solution. Another option, to obtain the limit cycle frequency, is to solve

$$\sum_{n=1(2)}^{\infty} \frac{2n\omega - n^3\omega^3}{n[(-3n^2\omega^2)^2 + (2n\omega - n^3\omega^3)^2]} = \frac{\pi\Delta}{4h} \tag{36}$$

for  $\omega$ . Strictly speaking, one should also check that the real part of the locus is negative but this is obviously the case for this simple example. Cases where it is not typically involve “unusual” transfer functions, and the DF solution may then also be a problem. For the relay with dead zone, two sets of loci must be plotted for the graphical approach because the two loci must be plotted for different values of  $\omega\Delta t = \theta$  say, and the solution is obtained when the given lines are intersected with the same  $\omega$  and  $\theta$  on the loci. Figure 11 shows  $A$  Loci of Equation (34) for different values of  $n$ . Table 1 shows the solution of Equation (36) for the relay with hysteresis for different values of  $n$ . Convergence is fast because the transfer function is a good low pass filter.

**Figure 11.**  $A$  Loci for different values of  $n$  for Equation (34) where  $h/\Delta = 2$ .

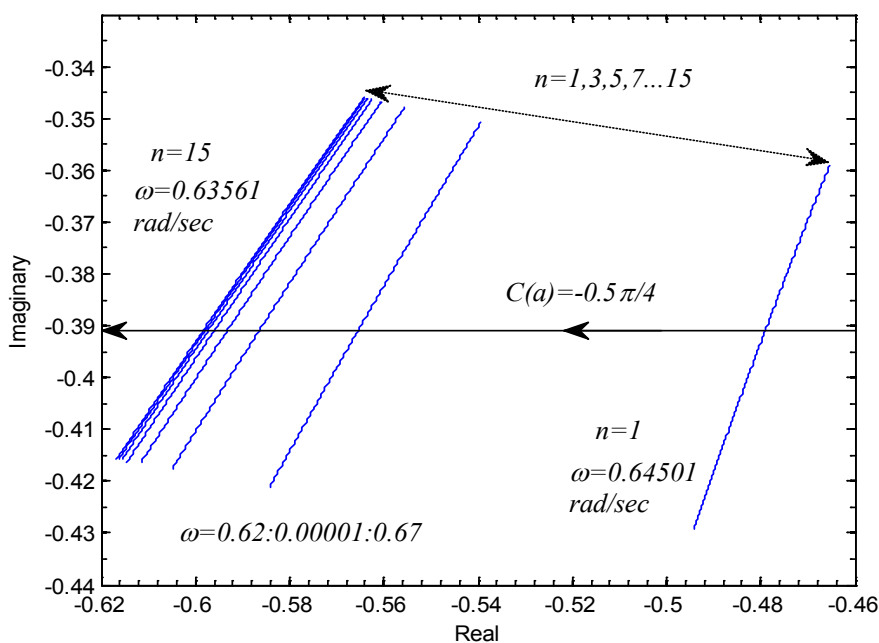


**Table 1.** Limit cycle frequencies for different values of  $n$  for Equation (34) where  $h/\Delta = 2$ .

$n$	$\omega$ (rad/s)	$n$	$\omega$ (rad/s)
1	0.6450	9	0.6359
3	0.6392	11	0.6357
5	0.6370	13	0.6356
7	0.6362	15	0.6356

**Example 2:** Consider the nonlinear system of Figure 6 with the integer order transfer function

$$G_2(s) = \frac{2 - s}{(s + 2)^2} \tag{37}$$

and an ideal relay. This transfer function is not a good filter so there is some distance between the  $A$  locus and Nyquist plots as seen in Figure 12. The frequency of the limit cycle using the  $A$  locus plot, as seen from Figure 12 is  $\omega = 2.8985$  rad/s for  $n=101$  and  $\omega = 3.4641$  rad/s from the Nyquist plot. The limit cycle is shown in Figure 13, which can be seen to be quite distorted, hence the quite large difference in the two frequencies.

**Figure 12.**  $A$  Loci and Nyquist diagram of  $G_2(j\omega)$  and plot of  $C(a)$ .

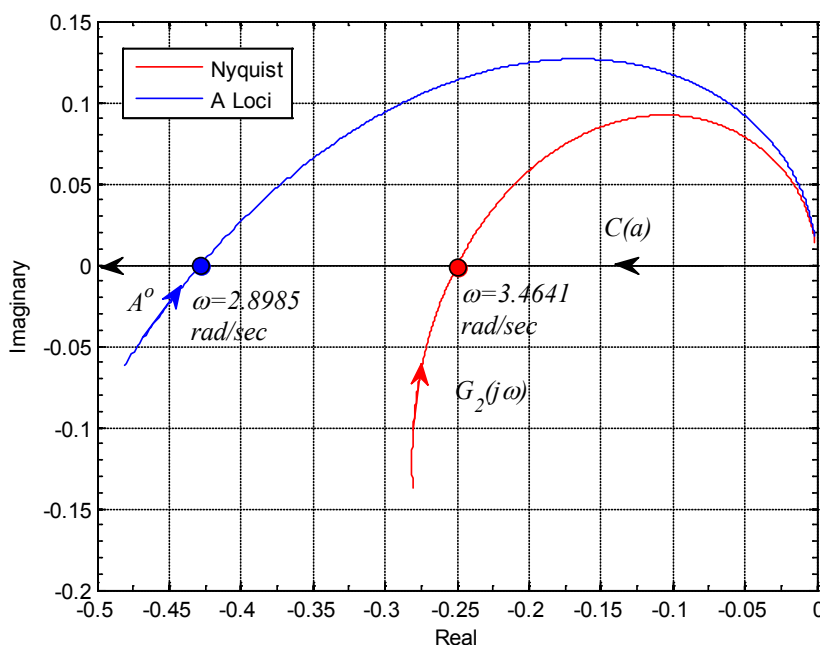
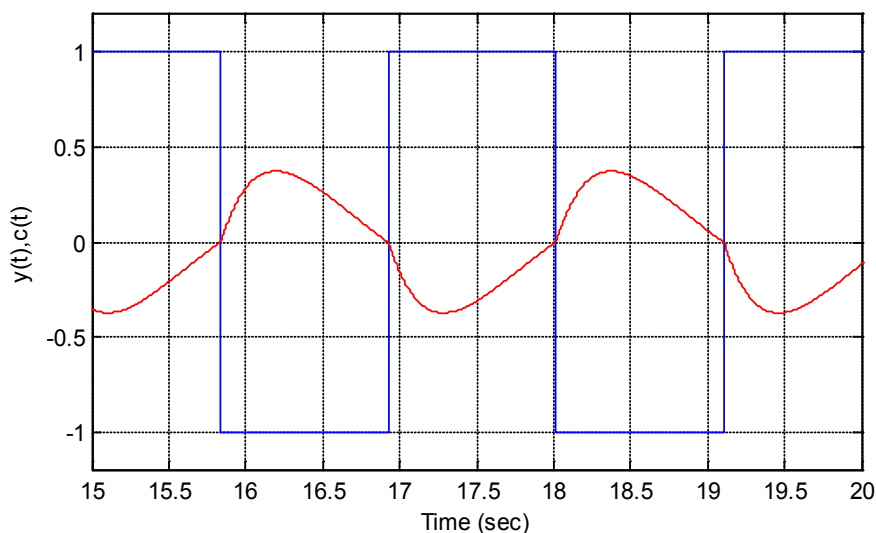


**Figure 13.** Time responses of closed loop system in Figure 6 with  $G_2(j\omega)$  and ideal relay ( $\omega = 2.88$  rad/s).

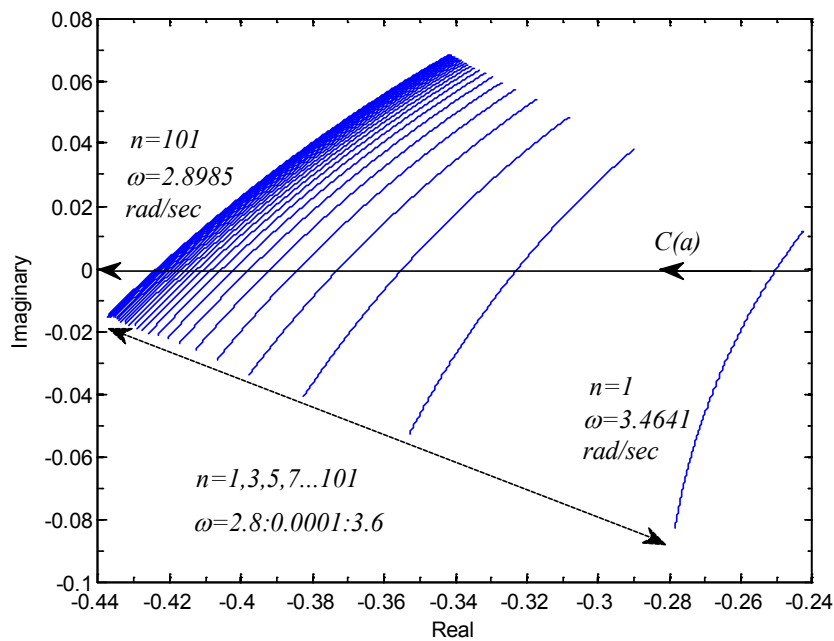


Solving the equation corresponding to Equation (36) for this example, for different values of  $n$ , gives Table 2. This shows, as expected, that larger values of  $n$  must be used to get the limit cycle frequency accurately.  $A$  Loci for different values of  $n$  are shown in Figure 14.

**Table 2.** Limit cycle frequencies for different values of  $n$  for Equation (37) where  $N(a)$  is an ideal relay.

$n$	$\omega$ (rad/s)	$n$	$\omega$ (rad/s)
1	3.4641	17	2.9578
3	3.2003	23	2.9398
5	3.0995	35	2.9218
7	3.0471	51	2.9107
9	3.0152	71	2.9038
11	2.9938	91	2.8998
13	2.9784	101	2.8985

**Figure 14.**  $A$  Loci for different values of  $n$  for Equation (37) where  $N(a)$  is an ideal relay.



**Example 3:** In this example, the Typskin loci for two plants, one is fractional order, with time delay are studied. These are:

$$G_{3i}(s) = \frac{3}{(s + 1)^2} e^{-s} \tag{38}$$

and

$$G_{3f}(s) = \frac{3}{s^{2.1} + 2s^{1.5} + 1} e^{-s} \tag{39}$$

The  $A$  Locus and Nyquist plots for  $G_{3i}(s)$  and  $G_{3f}(s)$  are shown in Figures 15 and 16, respectively.

From the figures, the exact limit cycle frequencies are 1.27 rads/s and 0.86 rads/s, respectively, for the integer order and fractional order plants.

Figure 15. A Loci and Nyquist diagram of  $G_{3i}(j\omega)$ .

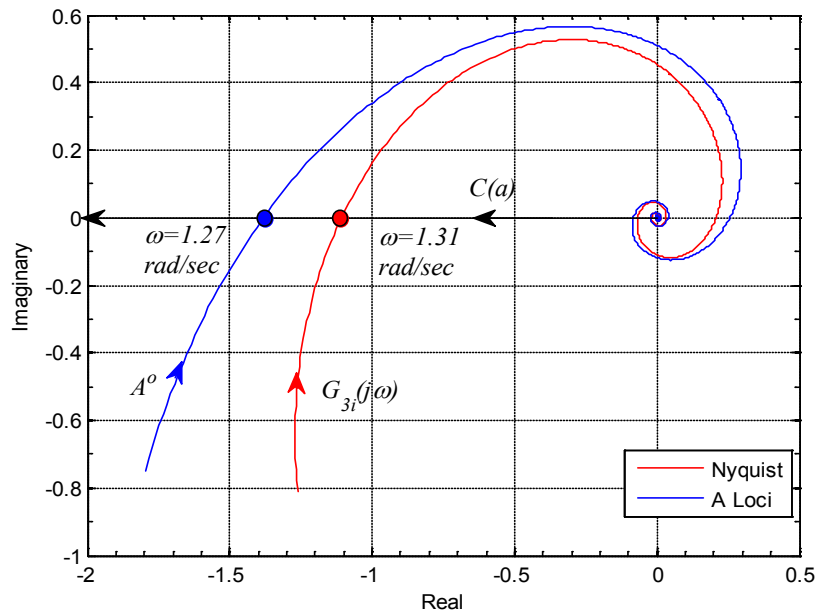
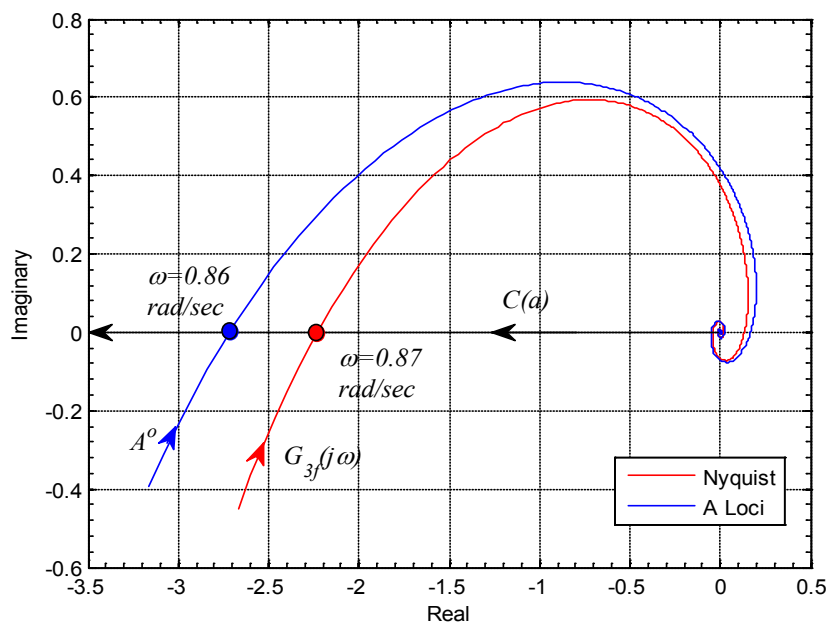


Figure 16. A Loci and Nyquist diagram of  $G_{3f}(j\omega)$ .



Example 4: Consider Figure 6 with the fractional order plant

$$G_4(s) = \frac{2}{s^{3.6} + 3s^{2.4} + 3s^{1.2} + 1} \tag{40}$$

Assume that the nonlinear system includes a relay with no dead zone. The  $A$  Locus, and the  $C(a)$  loci for the ideal relay and relay with hysteresis, having  $h/\Delta = 2$ , are shown in Figure 17.

Figure 17. A Loci of  $G_4(j\omega)$  and plot of  $C(a)$

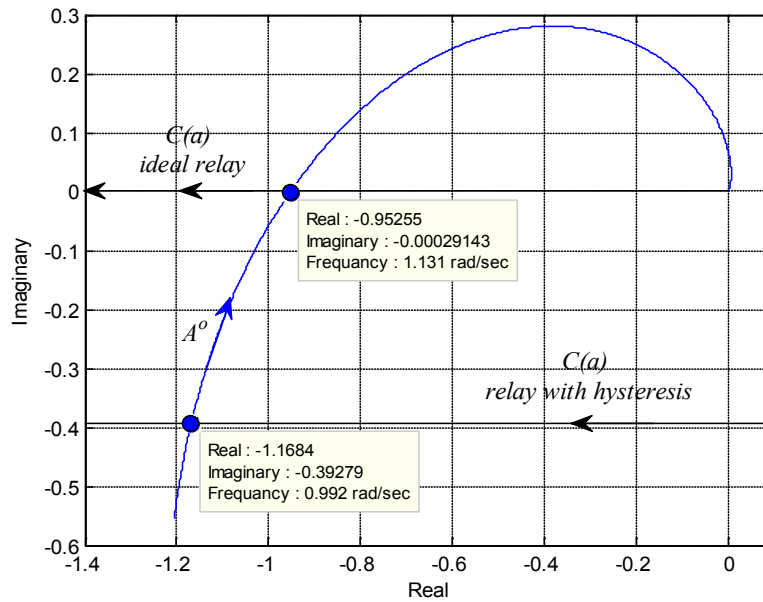
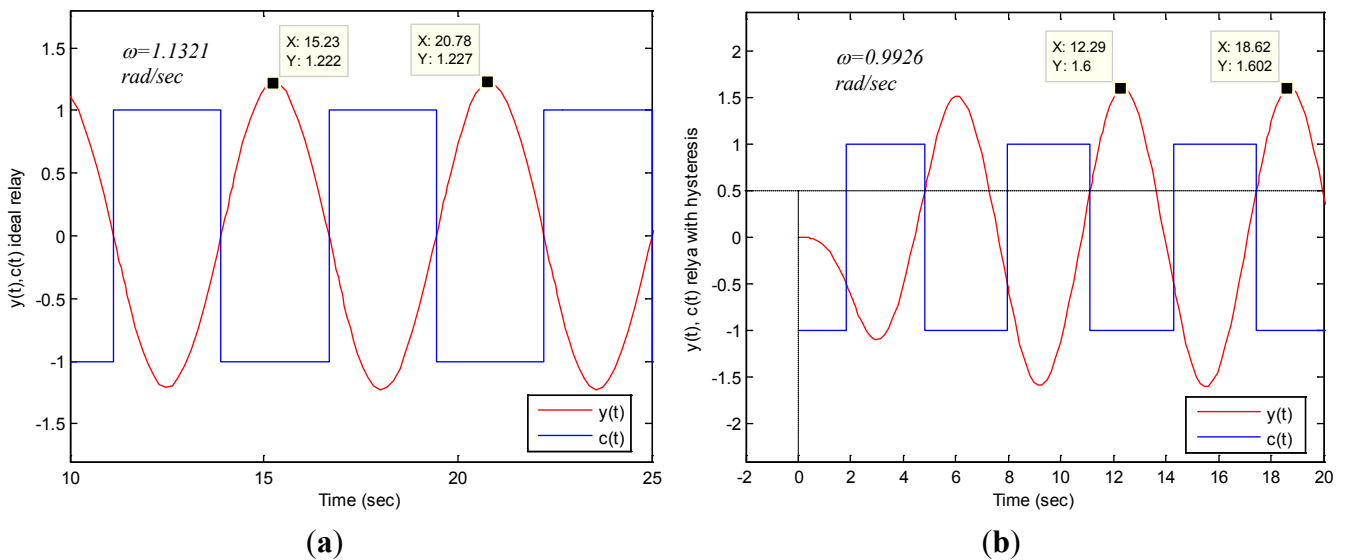


Figure 18 shows the time responses for the ideal relay and relay with hysteresis. The limit cycle frequencies are  $\omega = 1.1321$  rad/s and  $\omega = 0.9681$  rad/s, respectively.

It can be shown using the approximate DF theory that a necessary but not sufficient criterion for stability of a limit cycle is that the intersection between  $G(j\omega)$  and  $C(a)$  should be as shown in Figure 15. That is, if one moves along  $G(j\omega)$  in the direction of increasing frequency then at the point of intersection increasing amplitude on the  $C(a)$  locus will lie to the left.

Figure 18. Time responses of closed loop system in Figure 6 with  $G_4(j\omega)$  (a) ideal relay (b) relay with hysteresis.

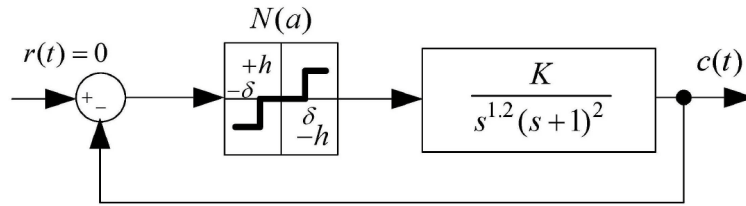


Example 5: Let us consider the transfer function

$$G_5(s) = \frac{K}{s^{1.2}(s + 1)^2} \tag{41}$$

in a feedback loop having a relay with dead zone as shown in Figure 19.

**Figure 19.** A nonlinear feedback system having relay with dead zone.

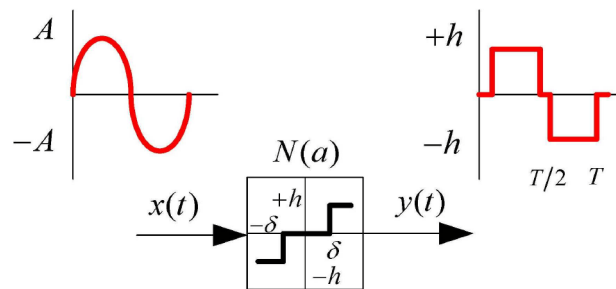


The DF for a relay with dead zone only, that is for  $a > \delta$ ,  $\Delta = 0$  is

$$N(a) = \frac{4h(a^2 - \delta^2)^{1/2}}{a^2\pi} \tag{42}$$

and its input and output waveforms are shown in Figure 20.

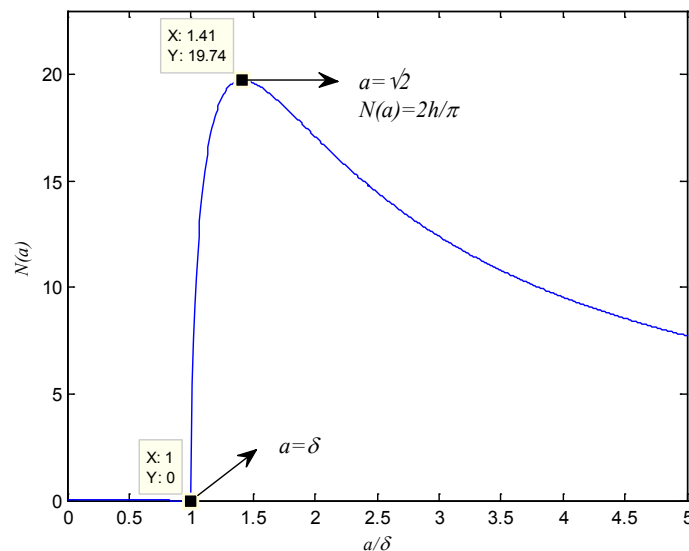
**Figure 20.** The diagram of the relay with dead zone.



The graph of  $N(a)$  is shown in Figure 21 where  $\delta = 1$  and it can easily be shown by differentiation that it has a maximum of  $2h/\pi\delta$  for  $a = \delta\sqrt{2}$ . For the transfer function of Equation (41), one can write

$$G_5(j\omega) = \frac{K}{(j\omega)^{1.2}(1 + j\omega)^2} \tag{43}$$

**Figure 21.** Graphical illustration of Describing Function(DF) (relay with dead zone) against  $a/\delta$  with  $h = \pi$ .

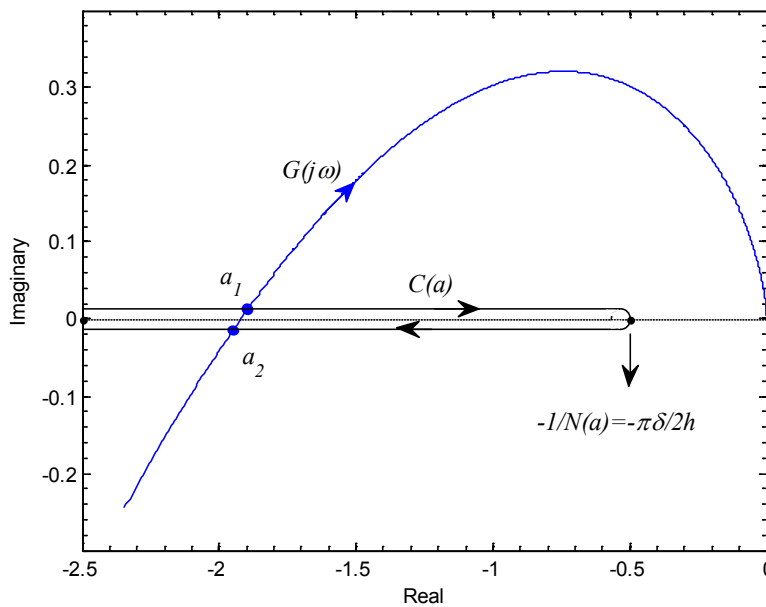


The real and imaginary parts of the denominator of  $G_5(j\omega)$  are  $-0.309\omega^{1.2} - 1.902\omega^{2.2} + 0.309\omega^{3.2}$  and  $0.9510\omega^{1.2} - 0.6180\omega^{2.2} - 0.9510\omega^{3.2}$ , respectively. Thus, Equation (14), which is  $1 + N(a)G(j\omega) = 0$  gives

$$-0.309\omega^{1.2} - 1.902\omega^{2.2} + 0.309\omega^{3.2} + \frac{4hK(a^2 - \delta^2)^{1/2}}{a^2\pi} + j(0.9510\omega^{1.2} - 0.6180\omega^{2.2} - 0.9510\omega^{3.2}) = 0 \tag{44}$$

Figure 22 shows a plot of  $G(j\omega)$  and  $C(a)$  from which it is seen that the latter travels along the negative real axis from minus infinity as  $a$  increases to a maximum of  $-\pi\delta/2h$  and then returns. Thus, there are two intersections with  $G(j\omega)$  and according to the above criterion only the larger amplitude one corresponds to a stable limit cycle.

**Figure 22.** Nyquist plot of  $G(j\omega)$  and  $C(a)$  (relay with dead zone).



### 3.2.1. Analysis of Limit Cycle Existence According to Compensator Gain

The above transfer function for  $K = 1$  crosses the negative real axis at a frequency of 0.7265 rad/s and its magnitude is given by:

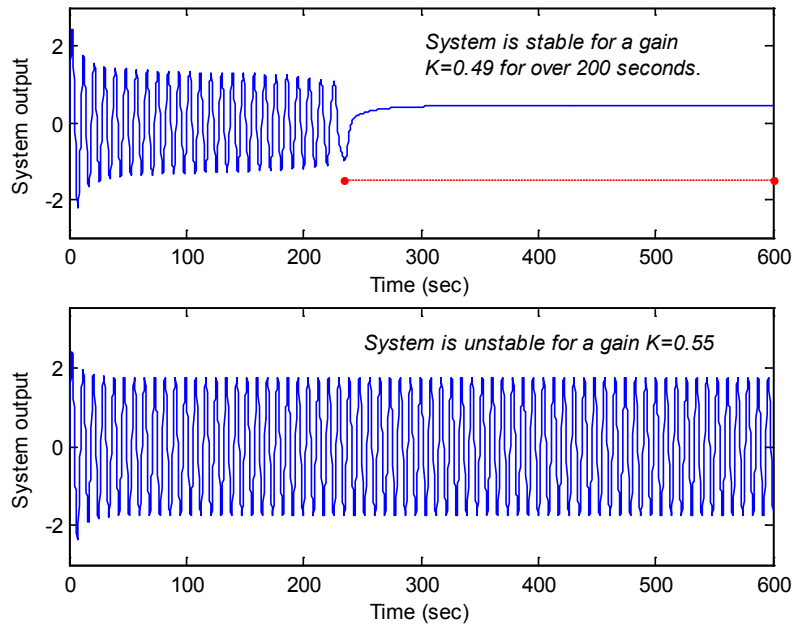
$$\frac{1}{(j\omega)^{1.2}(j\omega + 1)^2} = \frac{1}{\omega^{1.2}(1 + \omega^2)} \Big|_{\substack{\angle G(j\omega) = -180^\circ \\ \omega = 0.7265}} = 0.959 \tag{45}$$

An intersection with  $C(a)$  will thus only occur if

$$0.959KN(a)_{max} > 1 \tag{46}$$

Taking  $\delta = 1$ ,  $h = \pi$  for the relay gives  $N(a)_{max} = 2$ , so that for stability  $K < 0.521$ . Figure 23 shows simulation results for  $K = 0.49$  and  $0.55$ . The former is seen to be stable and a limit cycle exists for the latter. In the simulation, a limit cycle developed for  $K$  just greater than 0.49. Thus, although both results are approximate, there is good agreement.

**Figure 23.** Time responses of closed loop system in Figure 19 with Equation (43) and relay with dead zone for  $K = 0.49$  and  $0.55$



3.2.2. Analysis of Limit Cycle Existence According to Fractional Order Dynamics

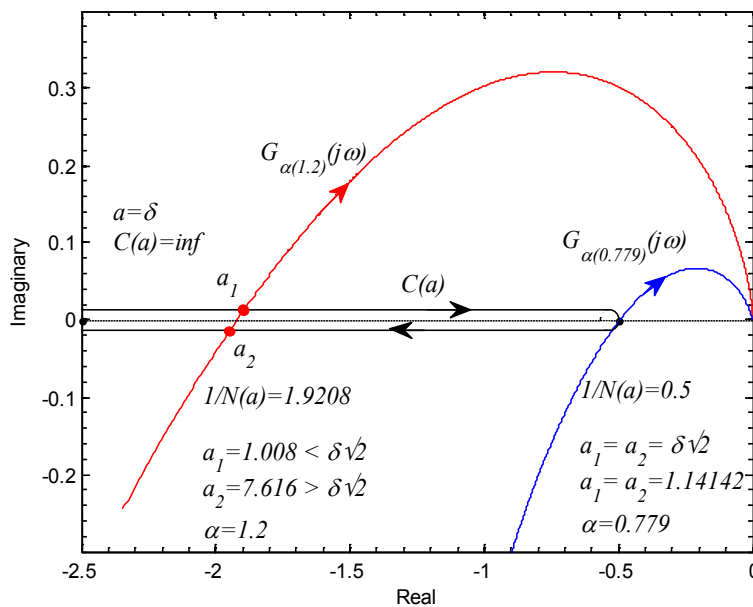
In this example, the effect of the change in order of a fractional integrator on the feedback loop stability is investigated.

**Example 6:** Consider the control system of Figure 19 with the fractional order plant

$$G_{\alpha}(s) = \frac{2}{s^{\alpha}(s + 1)^2} \tag{47}$$

where  $\alpha$  is the fractional order of the integrator  $1/s^{\alpha}$ . The relay is again taken to have  $\delta = 1, h = \pi$ . The  $G(j\omega)$  loci for  $\alpha = 1.2$  and  $\alpha = 0.779$ , which passes through  $-0.5$ , are shown in Figure 24.

**Figure 24.** The  $G_{\alpha}(j\omega)$  loci for  $\alpha = 1.2$  and  $\alpha = 0.779$ .



Two values of amplitude can be found from the chosen value of alpha and the corresponding limit cycle frequency from the equation

$$\frac{2}{\omega^\alpha(1 + \omega^2)} = \frac{-a^2}{4(a^2 - 1)^{1/2}} \tag{48}$$

For example, for  $\alpha = 1.2$  then  $\omega = 0.7265$  rad/s from  $\arg[G(j\omega)] = -\pi$ , and the two values of amplitude are found from  $a^4 - 58.878a^2 + 58.878 = 0$  giving  $a_1 = 1.008$  and  $a_2 = 7.616$ . Also shown in Figure 25 and Table 3 are the frequencies and corresponding amplitudes at  $\arg[G(j\omega)] = -\pi$  as a function of  $\alpha$ .

**Figure 25.** Nyquist plots for different values of  $\alpha$  for Equation (47) where  $N(a)$  is a relay with dead zone.

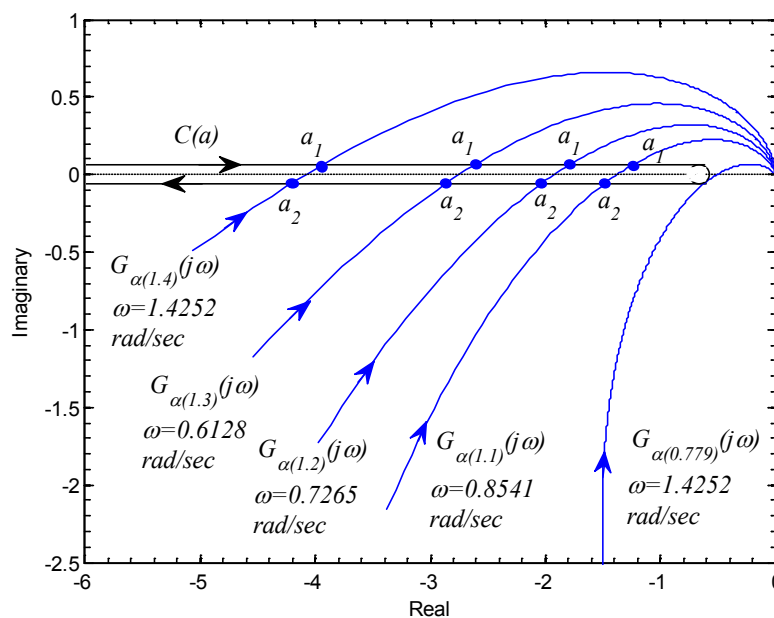


**Table 3.** The frequencies and corresponding amplitudes at  $\arg[G(j\omega)] = -180^\circ$  as a function of  $\alpha$ .

$\alpha$ (Fractional Order)	$\omega$ rad/s (The Frequency at $\arg[G(j\omega)] = -\pi$ )	$a$ (The Amplitude at $\arg[G(j\omega)] = -\pi$ )
0.779	1.4252	$a_1 = 1.141, a_2 = 1.141$
1.1	0.8541	$a_1 = 1.0176, a_2 = 5.407$
1.2	0.7265	$a_1 = 1.008, a_2 = 7.616$
1.3	0.6128	$a_1 = 1.004, a_2 = 10.946$
1.4	0.5095	$a_1 = 1.001, a_2 = 16.294$

**Example 7:** Here, example 5 shown in Figure 19 is again considered to illustrate the Tsytkin method. The relay parameters were again taken as  $\delta = 1, h = \pi$  to allow comparison of the results with those obtained using the DF method and initially  $K$  was taken equal to 1. The required  $A$  loci plots  $A_G^o(0, \omega) - A_G^o(\omega\Delta t, \omega)$  and  $A_G^o(0, \omega) - A_G^o(-\omega\Delta t, \omega)$  were plotted for a selection of values of  $\Delta t$  as shown in Figure 26, and the values of  $\omega$  and  $\Delta t$  were recorded where they met the lines  $-\pi\delta/2h$  and  $\pi\delta/2h$ , respectively. Table 4 shows recorded values of  $\omega$  and  $\Delta t$  for  $K = 1$ .

Figure 26. A loci for graphical solution for  $K = 1$ .

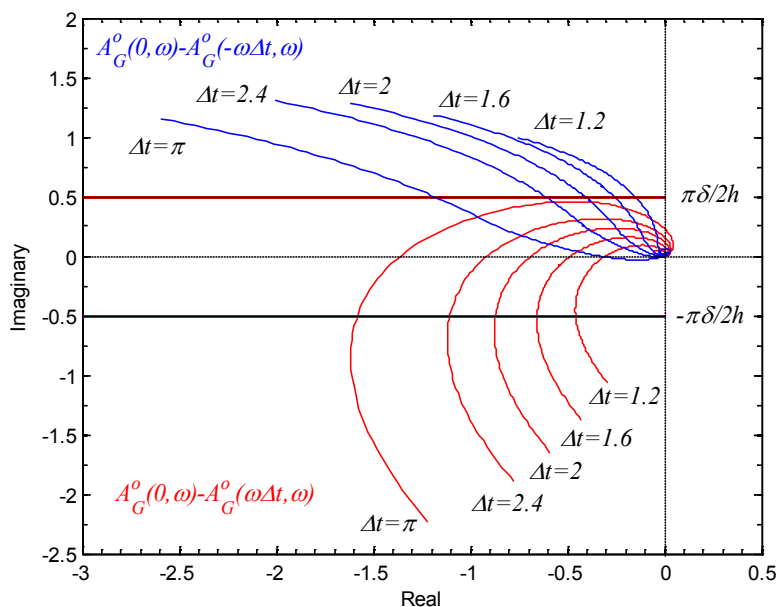
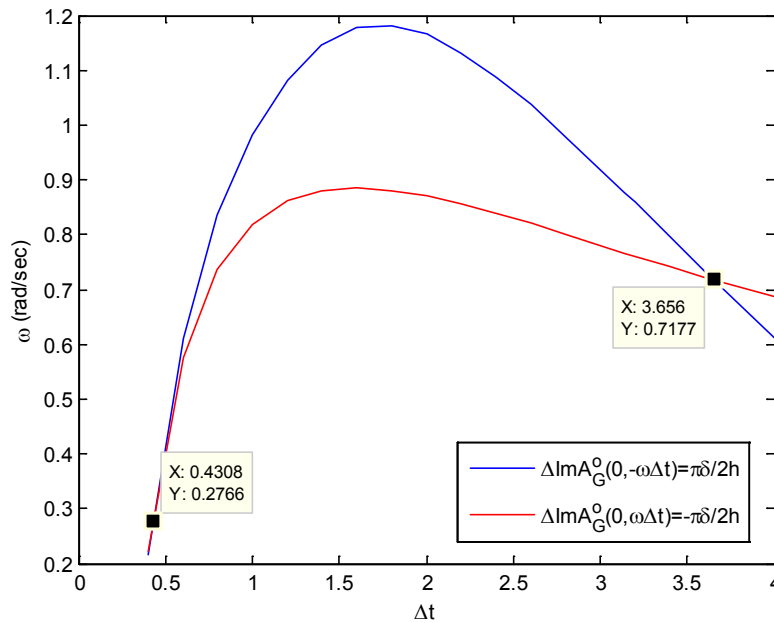


Table 4. Recorded values of  $\omega$  and  $\Delta t$  for  $K = 1$ .

$\Delta t$	$\omega$ rad/s	$\omega$ rad/s
	(Solution from $A_G^0(0, \omega) - A_G^0(\omega\Delta t, \omega) = -\pi\delta/2h$ )	(Solution from $A_G^0(0, \omega) - A_G^0(-\omega\Delta t, \omega) = \pi\delta/2h$ )
0.4	0.222	0.216
0.6	0.577	0.61
0.8	0.736	0.835
1	0.818	0.983
1.2	0.861	1.083
1.4	0.881	1.146
1.6	0.886	1.177
1.8	0.881	1.181
2.0	0.871	1.165
2.2	0.856	1.132
2.4	0.838	1.088
2.6	0.82	1.037
2.8	0.8	0.98
3.14	0.767	0.878
3.2	0.761	0.859
3.4	0.741	0.797
3.6	0.723	0.735
3.8	0.704	0.673
4	0.687	0.612

The values of  $\omega$  and  $\Delta t$  which satisfy both relationships  $A_G^0(0, \omega) - A_G^0(\omega\Delta t, \omega) = -\pi\delta/2h$  and  $A_G^0(0, \omega) - A_G^0(-\omega\Delta t, \omega) = \pi\delta/2h$  can then be found by plotting the values given in Table 4 in  $(\Delta t, \omega)$  plane as shown in Figure 27. From Figure 27, it was found that there are two solutions one is  $(\Delta t, \omega) = (3.656 \text{ s}, 0.7177 \text{ rad/s})$  and the other is  $(\Delta t, \omega) = (0.4308 \text{ s}, 0.2766 \text{ rad/s})$ .

Figure 27. Plots of recorded values given in Table 4.



The procedure was repeated for decreasing values of  $K$  and the results are given in Table 5 which shows the frequency and pulse width of the stable and unstable limit cycles. There are two frequency values for each  $K$  and larger one corresponds to a stable limit cycle.

Table 5. The frequency and pulse width of the stable and unstable limit cycles for different values of  $K$ .

$K$	$\omega$	$\Delta t$	$\theta = \omega\Delta t$
1	0.7177	3.656	2.623
	0.2766	0.4308	0.119
0.6	0.7142	3.055	2.181
	0.5712	1.044	0.596
0.55	0.7204	2.664	1.919
	0.6103	1.246	0.760
0.52	0.7152	2.438	1.7437
	0.6411	1.444	0.9257
0.49	No solution. System is stable		

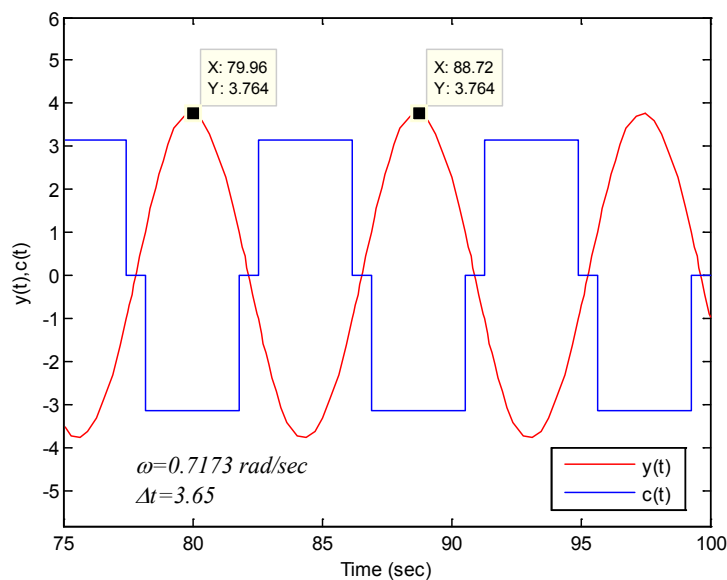
The value of  $K$  for which no solution was possible, and thus the system was stable, was 0.49. The results obtained from simulation, DF and  $A$  locus methods for comparison are given in Table 6 where it can be seen that the system is stable for  $K \leq 0.52$  according to DF method and it is stable for  $K \leq 0.49$  according to simulation and  $A$  locus methods.

Time domain simulation using Figure 19 is shown in Figure 28 which is the stable limit cycle obtained from a simulation with  $K = 1$ . Limit cycle frequency and pulse width are computed as  $\omega = 0.7173$  rad/s and  $\Delta t = 3.65$ , respectively.

**Table 6.** Results from simulation, DF and *A* Locus methods.

<i>K</i>	Method	$\omega$	$\Delta t$	$\theta = \omega \Delta t$
1	Simulation	0.7173	3.65	2.618
	DF	-	-	-
	<i>A</i> Locus	0.7265	3.57	2.59
0.6	Simulation	-	-	-
	DF	0.7265	2.88	2.09
	<i>A</i> Locus	0.7142	3.055	2.181
0.55	Simulation	0.7222	2.7	1.949
	DF	-	-	-
	<i>A</i> Locus	0.5712	1.044	0.596
0.52	Simulation	0.7204	2.664	1.919
	DF	0.6103	1.246	0.760
	<i>A</i> Locus	0.7140	2.4	1.713
0.49	Simulation	No limit cycle. System is stable.		
	DF	No solution. System is stable.		
	<i>A</i> Locus	0.7152	2.438	1.743
0.49	Simulation	0.6411	1.444	0.9257
	DF	No solution. System is stable.		
	<i>A</i> Locus	No solution. System is stable.		

**Figure 28.** Time responses of closed loop system in Figure 19 for  $K = 1$  with  $G_s(j\omega)$  and relay with dead zone.



#### 4. Conclusions

In this paper, after a brief review of the DF method the computation of the  $A$  locus for a fractional order plant has been studied. The  $A$  locus method is important as it allows calculation of the exact limit cycle frequency in a relay control system. For the fractional order plant, the  $A$  locus has to be computed by summing terms of a series and taking one term only is the equivalent of the DF method. Several examples have been given showing applications of the DF and  $A$  loci methods to the computation of limit cycles in fractional order plants and the results compared. It is known that the calculations to find the limit cycles in feedback systems containing relay type characteristics can be done using either time domain or frequency domain methods. Therefore, the problem of the calculation of limit cycles in a system with a relay with dead zone and a fractional order transfer function using time domain approach can be considered as future work and comparing the exact frequency domain approach with the approximate time domain solution can provide useful results.

#### Author Contributions

The idea of writing a paper on limit cycles analysis for nonlinear systems with fractional order plants comes from Derek P. Atherton and Nusret Tan. The organization of the paper, writing and selection of examples are done by Derek P. Atherton, Nusret Tan and Celaleddin Yeroğlu. Gürkan Kavuran and Ali Yüce done simulations.

#### Conflicts of Interest

The authors declare no conflict of interest.

#### References

1. Sun, H.; Song, X.; Chen, Y.Q. A class of fractional order dynamic systems with fuzzy order. In Proceedings of the 8th World Congress on Intelligent Control and Automation, Jinan, China, 6–9 July 2010; pp. 197–201.
2. Xue, D.; Chen, Y.Q. A comparative introduction of four fractional order controllers. In Proceedings of the 4th World Congress on Intelligent Control and Automation, Shanghai, China, 10–14 June 2002; pp. 3228–3235.
3. Oustaloup, A.; Melchior, P.; Lanusse, P.; Cois, O.; Dancla, F. The CRONE toolbox for MATLAB. In Proceedings of the 2000 IEEE International Symposium on Computer Aided Control System Design, Anchorage, AK, USA, 25–27 September 2000; pp. 190–195.
4. Valerio, D.; da Costa, J.S. Ninteger: A non-integer control toolbox for Matlab. In Proceedings of the 1st IFAC Workshop on Fractional Differentiation and Its Applications, Bordeaux, France, 19–21 July 2004.
5. Tepljakov, A.A.; Petlenkov, E.; Belikov, J. FOMCON: Fractional-order modeling and control toolbox for Matlab. In Proceedings of the 18th International Conference, Mixed Design of Integrated Circuits and Systems, Gliwice, Poland, 16–18 June 2011; pp. 684–689.
6. Xue, D.; Chen, Y.Q.; Atherton, D.P. *Feedback Control Systems—Analysis and Design with MATLAB 6*; Springer-Verlag: London, UK, 2002.

7. Podlubny, I. Fractional-order systems and  $PI^\lambda D^\mu$  controllers. *IEEE Trans. Autom. Control* **1999**, *44*, 208–214.
8. Sabatier, J.; Poullain, S.; Latteux, P.; Thomas, J.L.; Oustaloup, A. Robust speed control of a low damped electromechanical system based on CRONE control: Application to a four mass experimental test bench. *Nonlinear Dyn.* **2004**, *38*, 383–400.
9. Valério, D.; da Costa, J.S. Time domain implementation of fractional order controllers. *IEEE Proc. Control Theory Appl.* **2005**, *152*, 539–552.
10. Machado, J. Discrete-time fractional-order controllers. *Fract. Calc. Appl. Anal.* **2001**, *4*, 47–66.
11. Monje, C.A.; Vinagre, B.M.; Feliu, V. Tuning and auto-tuning of fractional order controllers for industry applications. *Control Eng. Pract.* **2008**, *16*, 798–812.
12. Chen, Y.Q.; Ahn, H.S.; Podlubny, I. Robust stability check of fractional order linear time invariant systems with interval uncertainties. *Signal Process.* **2006**, *86*, 2611–2618.
13. Tan, N.; Ozguven, O.F.; Ozyetkin, M.M. Robust stability analysis of fractional order interval polynomials. *ISA Trans.* **2009**, *48*, 166–172.
14. Atherton, D.P. *An Introduction to Nonlinearity in Control Systems*, Ventus Publishing Aps., 2011. Available online: <http://bookboon.com/en/an-introduction-to-nonlinearity-in-control-systems-ebook> (accessed on 31 March 2014).
15. Atherton, D.P. *Nonlinear Control Engineering: Describing Function Analysis and Design*; Van Nostrand Reinhold: London, UK, 1975.
16. Atherton, D.P. *Stability of Nonlinear Systems*; Research Studies Press, John Wiley: Chichester, NH, USA, 1981.
17. Tsympkin, Y.Z. *Relay Control Systems*; Cambridge University Press: England, UK, 1984.
18. Das, S. *Functional Fractional Calculus for System Identification and Control*; Springer-Verlag: Berlin/Heidelberg, Germany, 2008.
19. Nonnenmacher, T.F.; Glöckle, W.G. A fractional model for mechanical stress relaxation. *Philos. Mag. Lett.* **1991**, *64*, 89–93.
20. Westerlund, S.; Ekstam, L. Capacitor theory. *IEEE Trans. Dielectr. Electr. Insul.* **1994**, *1*, 826–839.
21. Bagley, R.L.; Calico, R.A. Fractional order state equations for the control of viscoelastic structures. *J. Guid. Control Dyn.* **1991**, *14*, 304–311.
22. Skaar, S.B.; Michel, A.N.; Miller, R.K. Stability of viscoelastic control systems. *IEEE Trans. Autom. Control* **1988**, *33*, 348–357.
23. Ichise, M.; Nagayanagi, Y.; Kojima, T. An analog simulation of non-integer order transfer functions for analysis of electrode processes. *J. Electroanal. Chem. Interfacial Electrochem.* **1971**, *33*, 253–265.
24. Hartley, T.T.; Lorenzo, C.F. Dynamics and control of initialized fractional-order systems. *Nonlinear Dyn.* **2002**, *29*, 201–233.
25. Sun, H.; Abdelwahab, A.; Onaral, B. Linear Approximation of transfer function with a pole of fractional power. *IEEE Trans. Autom. Control* **1984**, *29*, 441–444.
26. Mandelbrot, B. Some noises with  $1/f$  spectrum, a bridge between direct current and white noise. *IEEE Trans. Inf. Theory* **1967**, *13*, 289–298.

27. Goldberger, A.L.; Bhargava, V.; West, B.J.; Mandell, A.J. On the mechanism of cardiac electrical stability. *Biophys. J.* **1985**, *48*, 525–528.
28. Magin, R.L. *Fractional Calculus in Bioengineering*; Begell House Publishers: CT, USA, 2006.
29. Hartley, T.T.; Lorenzo, C.F.; Qammar, H.K. Chaos in a fractional order Chua system. *IEEE Trans. Circuits Syst. I* **1995**, *42*, 485–490.
30. Monje, C.A.; Chen, Y.Q.; Vinagre, B.M.; Xue, D.; Feliu, V. *Fractional-Order Systems and Controls: Fundamentals and Applications*; Springer: London; New York, 2010.
31. Podlubny, I. *Fractional Differential Equations*; Academic Press: San Diego, CA, USA, 1999.
32. Krajewski, W.; Viaro, U. A method for the integer-order approximation of fractional-order systems. *J. Frankl. Inst.* **2014**, *351*, 555–564.
33. Vinagre, B.M.; Podlubny, I.; Hernández, A.; Feliu, V. Some approximations of fractional order operators used in control theory and applications. *Fract. Calc. Appl. Anal.* **2000**, *3*, 231–248.
34. Chen, Y.Q.; Petráš, I.; Xue, D. Fractional order control—A tutorial. In Proceedings of the 2009 American Control Conference, Hyatt Regency Riverfront, St. Louis, MO, USA, 10–12 June 2009; pp. 1397–1411.
35. Krishna, B.T. Studies on fractional order differentiators and integrators: A survey. *Signal Process.* **2011**, *91*, 386–426.
36. Djouambi, A.; Charef, A.; Voda, A. Numerical Simulation and Identification of Fractional Systems using Digital Adjustable Fractional Order Integrator. In Proceedings of the 2013 European Control Conference (ECC), Zürich, Switzerland, 17–19 July 2013; pp. 2615–2620.
37. Oustaloup, A.; Levron, F.; Mathieu, B.; Nanot, F.M. Frequency band complex noninteger differentiator: Characterization and synthesis. *IEEE Trans. Circuit Syst. I Fundam. Theory Appl.* **2000**, *47*, 25–39.
38. Carlson, G.E.; Halijak, C.A. Approximation of fractional capacitors  $(1/s)^{1/n}$  by a regular Newton process. *IEEE Trans. Circuit Theory* **1964**, *11*, 210–213.
39. Matsuda, K.; Fujii, H.  $H_\infty$ -optimized wave-absorbing control: Analytical and experimental results. *J. Guid. Control Dyn.* **1993**, *16*, 1146–1153.
40. Charef, A.; Sun, H.H.; Tsao, Y.Y.; Onaral, B. Fractal system as represented by singularity function. *IEEE Trans. Autom. Control* **1992**, *37*, 1465–1470.
41. Duarte, V.; Costa, J.S. Time-domain implementations of non-integer order controllers. In Proceedings of the Control 2002, Aveiro, Portugal, 5–7 September 2002; pp. 353–358.
42. Ozyetkin, M.M.; Yeroglu, C.; Tan, N.; Tagluk, M.E. Design of PI and PID controllers for fractional order time delay systems. In Proceedings of the 9th IFAC workshop on Time Delay Systems, Prague, Czech, 7–9 June 2010.
43. Atherton, D.P. Early developments in nonlinear control. *IEEE Control Syst.* **1996**, *16*, 34–43.